Geomorphology 445 (2024) 108970

Contents lists available at ScienceDirect

Geomorphology

journal homepage: www.journals.elsevier.com/geomorphology

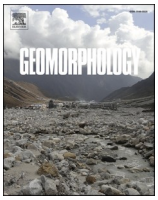

Cirques in the Transantarctic Mountains reveal controls on glacier formation and landscape evolution

Iestyn D. Barr [a,*], Matteo Spagnolo [b], Matt D. Tomkins [c]

[a] Department of Natural Sciences, Manchester Metropolitan University, Manchester, UK
[b] School of Geosciences, University of Aberdeen, Aberdeen, UK
[c] Department of Geography, University of Manchester, Manchester, UK

ARTICLE INFO

Keywords:
Antarctica
Glacial geomorphology
Landscape evolution
Cirque

ABSTRACT

In this study, we analyse the morphometry of cirques in the Transantarctic Mountains (TAM) to understand regional glacier formation and landscape evolution since the onset of Cenozoic glaciations. We find that, unlike most glacierised regions worldwide, aspect bias for cirques in the TAM is not particularly strong, indicating that glaciers were able to form and cirques develop on slopes with a variety of aspects. This is perhaps unsurprising, given that Antarctica's climate has been conducive to long-lived and extensive glaciation for many millions of years. Surprisingly, where cirques in the TAM show an aspect bias, this is typically towards the North, NW and/or NE, rather than favouring South-facing slopes where direct solar radiation is comparatively limited. This lack of a poleward aspect bias is unlike most cirque populations globally and indicates that total solar insolation was not a key control on where former glaciers in the TAM were able to initiate. Instead, we argue that prevailing wind directions played a dominant role in controlling the slopes on which past glacier development was favoured. Specifically, South-facing slopes in the TAM are directly exposed to katabatic winds which originate from the interior of the East Antarctic Ice Sheet (EAIS). These slopes are therefore susceptible to wind deflation, with snow and ice being redistributed to lee-side slopes where it can accumulate due to protection from the wind. For this reason, North, NE and/or NW facing slopes may have favoured glacier development, and therefore resulted in a concentration of cirques with these aspects. This evidence suggests that most cirques in the TAM are no older 34 Ma, as outward radiating winds from the continent's interior could only have prevailed when the EAIS was present (in some form). By contrast, the very highest (and likely oldest) cirques in the TAM have more varied aspects, indicating that they may have formed before katabatic winds came to dominate, and by extension, before widespread growth of the EAIS at 34 Ma, and could perhaps have formed as far back as 60 Ma. In general, we find that cirques in the TAM have similar dimensions to those in other regions globally, despite having been occupied by glacial ice for far longer. Thus, our findings support a growing body of evidence which suggests that cirque size and glacier occupation times are not directly coupled, though there is some evidence of spatial variability in cirque size which might relate to the differences in the dynamics of former glaciers.

1. Introduction

Cirques are topographic depressions formed (and largely shaped) by subglacial erosion. They reflect sites of former mountain glaciation and are ubiquitous in glaciated regions globally (Evans, 1977). Given their association with past mountain glaciers, their distribution and dimensions can provide palaeoenvironmental information, and they have been used for this purpose in many regions globally (e.g., Evans and Cox, 1995; Wallick and Principato, 2020; Zhang et al., 2020; Evans et al., 2021). Despite this, cirques in Antarctica (the most extensively glaciated continent on Earth) have received only limited research focus, partly because most are currently submerged beneath ice sheets (see Bo et al., 2009; Rose et al., 2013), and due to the historical paucity of high-resolution satellite imagery (particularly south of ~83°S) and digital elevation models (DEMs). Exceptions are Selby and Wilson (1971) who considered the possible age of a small number of cirques (n ~15) in the Wright Valley region of the Dry Valleys (part of the TAM), Andrews and LeMasurier (1973) who mapped and analysed a small number ($n = 8$) of very large cirques on the flanks of volcanoes in Marie Byrd Land (West Antarctica), Aniya and Welch (1981) who investigated the

* Corresponding author.
E-mail address: i.barr@mmu.ac.uk (I.D. Barr).

https://doi.org/10.1016/j.geomorph.2023.108970
Received 30 August 2023; Received in revised form 31 October 2023; Accepted 2 November 2023
Available online 10 November 2023

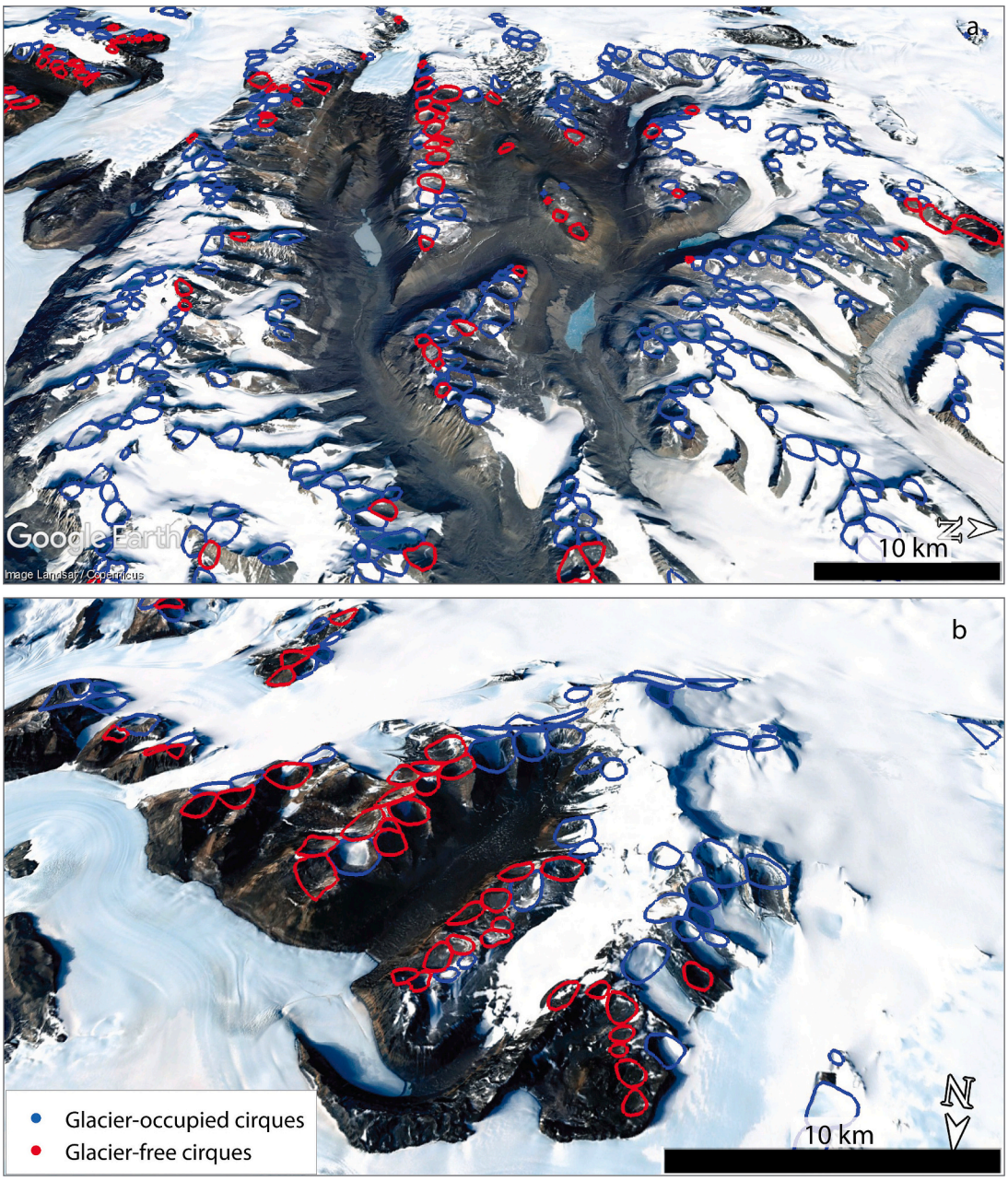

Fig. 1. Examples of glacier-occupied (blue polygons) and glacier-free (red polygons) cirques mapped in the Dry Valleys region of the Transantarctic Mountains. (a) Centred on 77.448°S, 161.654°E. (b) Centred on 77.845°S, 160.605°E.

morphometry of 56 (mostly ice free) cirques in the Victoria Valley system, part of the Dry Valleys, and Holmlund and Näslund (1994) who mapped and measured the dimensions of a small number ($n = 12$) of subglacial cirques and U-shaped valleys in Dronning Maud Land, East Antarctica.

Fortunately, over the past decade, various digital datasets of Antarctica's subglacial (e.g., Fretwell et al., **2013**) and surface (Howat et al., 2019) topography have become available and fundamentally changed the way the continent's land and ice are investigated (e.g., Jamieson et al., 2014; Small et al., 2021). The subglacial data are excellent for analysing large features (e.g., Rose et al., 2013) but are currently of insufficient spatial resolution to map and analyse comparatively small features such as cirques (typically <1 km in diameter, Barr and Spagnolo, 2015; Evans and Cox, 2017). By contrast, topographic models of the ice-free landscape are now of sufficient spatial resolution (<10 m) that features such as cirques can be mapped and analysed in unprecedented detail (Barr et al., 2022). In this study we use ice-free topographic data to analyse the morphology (aspect, size, and shape) of glacial cirques in the Transantarctic Mountains (TAM). This is the first study to analyse cirque morphology across the TAM to reveal information about Antarctica's glacial and landscape history during the Cenozoic.

1.1. Study area

The TAM extend >3000 km across the Antarctic continent, forming a geographic divide between the East and West (Elliot, 2013). Given their extent, the TAM cover ~30 degrees of latitude, and reach up to ~4500 m in elevation. They have existed for hundreds of millions of years (since the Neoproterozoic), but their current form is primarily Cenozoic in origin (Goodge, 2020). The most recent phase of the range's evolution involved Cenozoic uplift and volcanism alongside glaciation (Goodge,

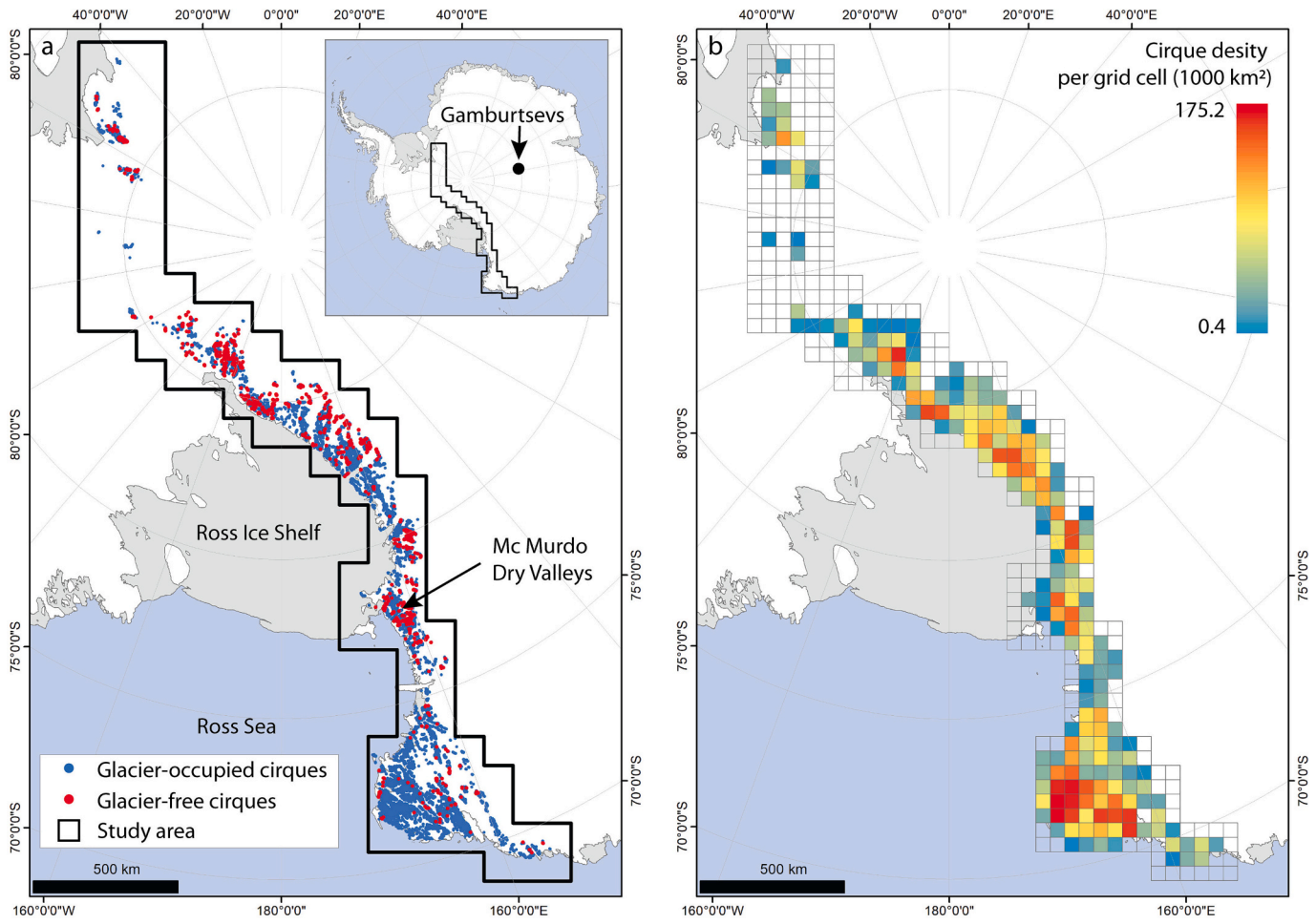

Fig. 2. (a) Cirques ($n = 14{,}060$) in the Transantarctic Mountains (as mapped by Barr et al., 2022), sub-divided into 'glacier-occupied' ($n = 12{,}768$) and 'glacier-free' ($n = 1292$) populations. (b) Cirque density (for the entire population) per 1000 km^2 (calculated per 50 km by 50 km grids square). Antarctic coastline data from Gerrish et al. (2021).

2020). The presence of Cenozoic glaciers in the mountains may have begun during the Late Palaeocene (~60–56 Ma) and continues to the present day (Barr et al., 2022). During this period, both warm- and cold-based mountain glaciers were present, before much of the range became shrouded by ice sheets at the Eocene-Oligocene boundary (~34 Ma, DeConto and Pollard, 2003). Thus, the mountains have a history of long-term glacier occupation, and are currently extensively glacierised. Despite this, there are large areas of exposed bedrock, not currently submerged beneath glacial ice (Goodge, 2020).

Cirques in the TAM are presumed to have formed during Cenozoic glaciations (Barr et al., 2022), though as with other cirque populations globally (Barr and Spagnolo, 2015), assigning a specific time of formation to these cirques is very difficult. It is possible that some date back to the onset of Cenozoic mountain glaciation, but others may be far younger (perhaps forming in the last few million years). Irrespective of their time of formation, it is likely that all cirques have experienced periods of active erosion and growth beneath warm-based ice masses, and periods of minimal growth beneath cold-based and therefore minimally erosive ice masses (Barr et al., 2019).

At present, climate in the TAM varies as a function of altitude, though cryo-arid conditions prevail, with mean monthly temperatures consistently below zero, even in coastal areas during the Austral Summer (Dec, Jan, Feb) (Wang et al., 2023). The region's weather is also dominated by katabatic winds which originate from the continent's interior and are funneled by ice topography through the valleys of the TAM (Parish and Bromwich, 1987, 2007). Though the strength of these winds reduces during summer, they are some of the strongest (up to 90 m/s) and most persistent low atmosphere winds on Earth (Parish and Bromwich, 2007).

2. Methods

The cirques analysed in this study were first mapped by Barr et al. (2022) using the Reference Elevation Model of Antarctica (REMA) Digital Surface Model (DSM), which has an 8 m spatial resolution and vertical error of <1 m (Howat et al., 2019). Where possible, this mapping was cross validated with existing cirque maps, though these are few and only cover small regions (see Selby and Wilson, 1971; Andrews and LeMasurier, 1973; Aniya and Welch, 1981; Holmlund and Näslund, 1994). Barr et al. (2022) mapped all cirques identifiable in the TAM, irrespective of their degree of glacier-coverage, i.e. since the mapping was performed from DSM data, all features with cirque-like topography were recorded, even if partially ice-covered (see examples in Fig. 1). Barr et al. (2022) subsequently divided this dataset of 14,060 cirques into 'glacier-occupied' ($n = 12{,}768$) and 'glacier-free' ($n = 1292$) populations (Fig. 2a). In the present study we use both populations (which can be downloaded as shapefiles from Barr et al., 2022). For the analysis of cirque aspect (i.e., orientation) all cirques in the dataset were

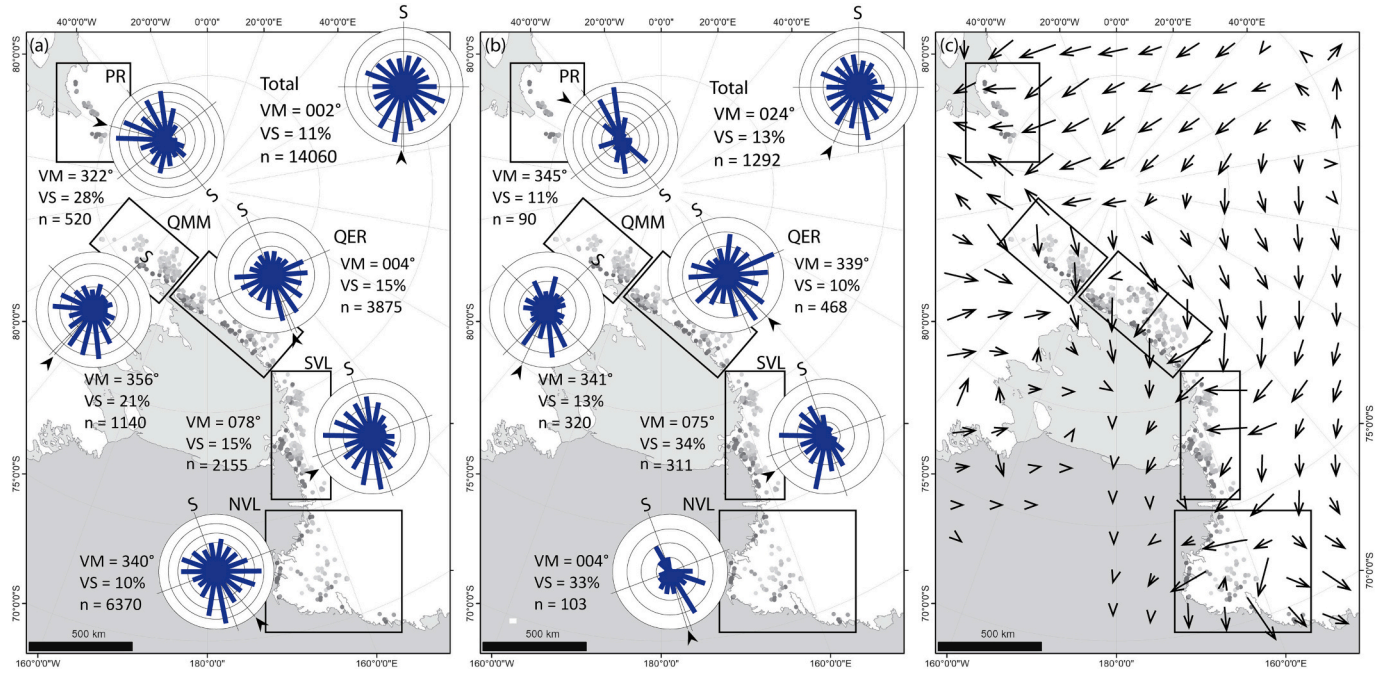

Fig. 3. Aspect frequency for (a) all cirques (n = 14,060) and (b) all glacier-free cirques (n = 1292) in the Transantarctic Mountains and for separate sub-regions. PR = The Pensacola Range; QMM = Queen Maud Mountains; QER = Queen Elizabeth Range; SVL = South Victoria Land; NVL = North Victoria Land. The vector strength (VS) and vector mean (VM) are also shown (the arrow in each rose diagram corresponds to the vector mean). Rose Diagrams are oriented according to each sub-region's approximate orientation. (c) Model representation of wind vectors across the TAM (from Parish and Cassano, 2003). Length of wind vectors corresponds to wind magnitude.

Table 1
Aspect Vector Mean (VM) and Vector Strength (VS) for cirques in the TAM and for different sub-regions of the TAM (for region acronyms see Fig. 2).

Sub-region	VM (°) all cirques	VS (%) all cirques	VM (°) glacier-free cirques	VS (%) glacier-free cirques	Approximate dominant wind vector (°)
All	002	11	024	13	Variable
PR	322	28	345	11	135
QMM	356	21	341	13	135
QER	004	15	339	10	225
SVL	078	15	075	34	270
NVL	340	10	004	33	225

considered, irrespective of their degree of ice cover, and aspect was measured as the orientation of the median axis, following Barr and Spagnolo (2013). Maximum altitude (Z_max) was also calculated for all cirques. For size and shape analysis, only 'glacier-free' cirques were considered, since cirques occupied by ice of unknown thickness are unlikely to yield robust information. For 'glacier-free' cirques, length (L), width (W), depth (H) minimum altitude (Z_min) and mean altitude (Z_mean) were calculated using an automated GIS tool, ACME, developed by Spagnolo et al. (2017). Additional calculated metrics for glacier-free cirques include the shortest distance to the modern coastline (Dist), following Oien et al. (2022), and the dominant lithology (accounting for greatest surface area of each cirque) using geological data from Cox et al. (2023).

3. Results

The 14,060 cirques are distributed throughout the TAM (Fig. 2a) but are most abundant and most densely spaced in areas immediately south and west of the Ross Sea and Ross Ice Shelf (Fig. 2b).

Table 2
Size and shape metrics for glacier-free cirques in the Transantarctic Mountains.

	Length (m)	Width (m)	Depth (m)
Min	199	138	79
Max	2445	3170	1271
Mean	779	833	413
Median	698	746	380
Sdev	361	416	196
Skew	1.14	1.40	1.09
10th percentile	398	408	198
90th percentile	1291	1390	683

3.1. Cirque aspect

The entire cirque population shows a weak Northern aspect bias, with a vector mean (VM) aspect of 002° (Fig. 3a). Vector strength (VS), which measures the degree of asymmetry in aspects, is only 11 % which suggests very weak aspect asymmetry, i.e., cirques do not show clearly preferred orientations. When cirques are divided into sub- populations (Fig. 3a), aspect shows a NW, North, or NE bias, but again this is typically very weak (Table 1). When the aspect of only glacier-free cirques are considered (Fig. 3b) very similar aspect trends are observed (Table 1).

3.2. Cirque size and shape

Glacier-free cirques in the TAM have L ranging from 199 m to 2445 m, with a mean of 779 m and median of 698 m; W ranging from 138 m to 3170 m, with a mean of 833 m and median of 746 m; and H ranging from 79 m to 1271 m, with a mean of 413 m and median of 380 m (Table 2). Frequency distributions for L, W and H are all unimodal, with positive skew (Fig. 4a). All size metrics (L, W, H) are positively correlated ($0.59 < r < 0.82$) (Table 3) indicating that long cirques also tend to be wide and deep. To investigate how shape varies with growth, cirque L, W, and H are plotted against size ($\sqrt[3]{LWH}$, see Evans, 2006a) (Fig. 4b). Based

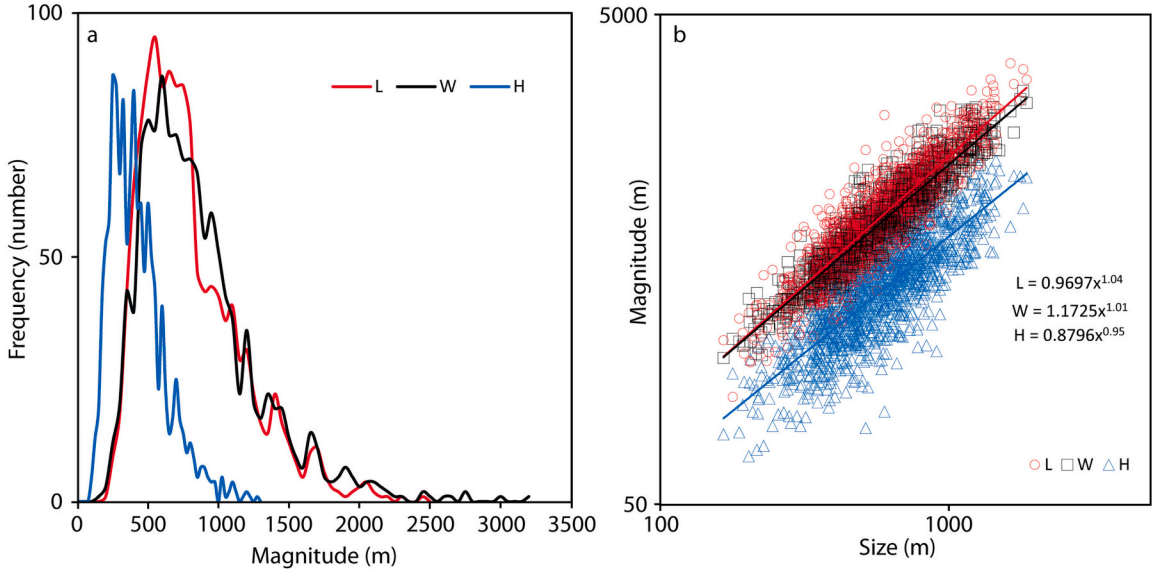

Fig. 4. (a) Frequency distributions for the Length (L), Width (W) and depth (H) of glacier-free cirques in the Transantarctic Mountains. (b) Allometric (double logarithmic) plot of L, W, and H against size ($\sqrt[3]{LWH}$) for each of these cirques.

Table 3
Pearson product moment correlation among attributes of glacier-free cirques in the Transantarctic Mountains.

	L	W	H
W	**0.81***		
H	**0.60***	**0.53***	
Lat	−0.07	0.00	**0.15***
Lon	**0.08***	0.04	**−0.12***
Z_min	−0.02	0.03	**0.10***
Z_max	**0.17***	**0.19***	**0.40***
Z_mean	0.04	**0.08***	**0.23***
Dist	−0.02	0.06	0.04

* Statistically significant relationships ($p < 0.01$).

on these plots, power exponents for L, W and H are 1.04, 1.01, and 0.95 respectively. This indicates that over time, cirques have grown roughly isometrically, though lengthening has slightly outpaced widening, which has slightly outpaced deepening. This comparatively isometric growth is atypical of cirque populations globally, which often show deepening substantially outpaced by lengthening and widening (see Barr and Spagnolo, 2015), and may reflect the varied lithology and structure of the TAM, as found for some large cirque populations elsewhere globally (e.g., Evans, 2006b; Barr and Spagnolo, 2013). In considering other relationships with cirque dimensions (Table 3), it is apparent that all size metrics (L, W, H) are positively correlated with Z_max ($0.16 < r < 0.41$, Fig. 5). W and H show a statistically significant positive correlation with Z_mean ($r = 0.08$ and 0.23, respectively). Only H shows a statistically significant correlation with Z_min ($r = 0.10$). These correlations suggest some relationship between cirque size and altitude, with the highest cirques also tending to be the largest and deepest.

3.3. Cirque size and shape with aspect

When the glacier-free cirques are divided into 8 aspect bins (N, NE, E, SE, S, SW, W, NW), one-way analysis of variance (ANOVA) reveals statistically significant variations in L (F-ratio = 8.6, F-crit = 2.0) and W (F-ratio = 3.7, F-crit = 2.0), and overall size (F-ratio = 4.2, F-crit = 2.0), but not H (F-ratio = 1.4, F-crit = 2.0). The NE-facing cirques show the largest mean L and W, and the South-facing group has the smallest (Table 4). The shallowest cirques (lowest H) are also found in the South-facing group, with the deepest in the East-facing group (Table 4). Despite these patterns, Fourier (harmonic) regression suggests that aspect related differences in cirque dimensions (L, W, and H) are not statistically significant.

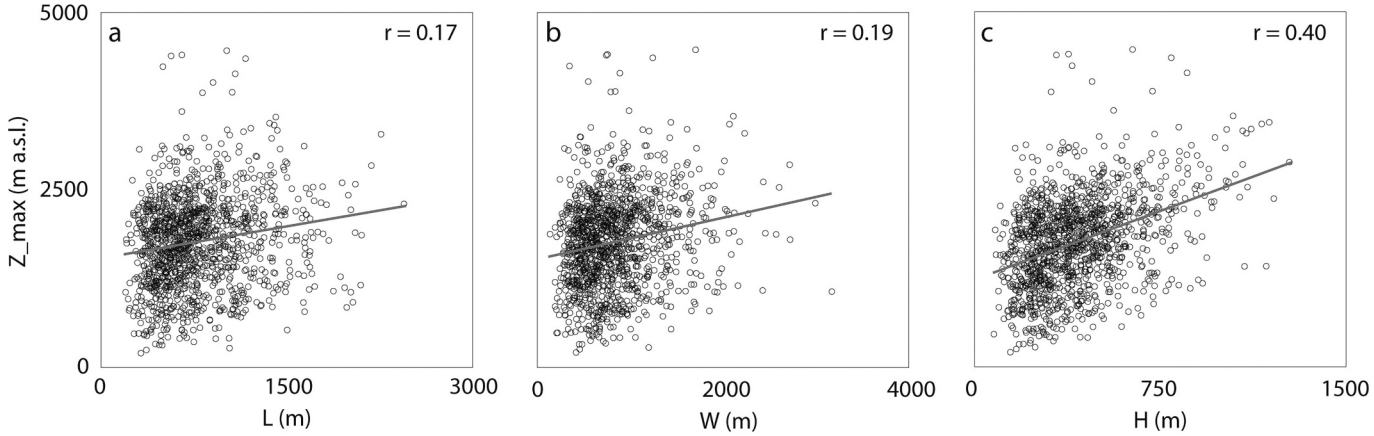

Fig. 5. Relationships between maximum altitude (Z_max) and size metrics (Length, Width, and depth) for all glacier-free cirques in the Transantarctic Mountains.

Table 4
Variation in size metrics with aspect for glacier-free cirques in the Transantarctic Mountains.

	Count	L (Mean)	L (SD)	W (Mean)	W (SD)	H (Mean)	H (SD)	Size (mean)	Size (SD)
N (338°-22°)	229	853	379	863	414	409	188	651	250
NE (23°-67°)	179	879	390	917	450	419	212	679	282
E (68°-112°)	168	818	360	870	417	440	189	664	260
SE (113°-157°)	158	687	331	789	408	418	199	598	261
S (158°-202°)	144	645	274	709	354	376	179	543	221
SW (203°-247°)	105	728	328	828	376	398	178	608	238
W (248°-292°)	129	784	365	801	396	419	215	627	280
NW (293°-337°)	180	761	359	842	447	414	199	629	282

3.4. Cirque lithology

When the glacier-free cirques are divided into 5 separate geological classes (Fig. 6), one-way ANOVA indicates statistically significant relationships for L (F-ratio = 9.0, F-crit = 2.4), W (F-ratio = 9.8, F-crit = 2.4), and H (F-ratio = 5.0, F-crit = 2.4). However, there are no consistent relationships to suggest clear geological controls on cirque size. For example, mean L and W are greatest for mixed sedimentary rocks and lowest for intrusive igneous rocks and volcanic igneous rocks (Fig. 6a and b), whereas mean H is greatest for igneous intrusive rocks and lowest for metamorphic rocks (Fig. 6c).

4. Discussion

4.1. Controls on glacier formation

Since cirques are formed in locations which favour the accumulation and preservation of snow and ice, the two key topoclimatic factors that determine cirque aspect are total solar insolation and prevailing wind directions (Evans, 1977), although topography and geological structure play a role (Gordon, 2001; Bathrellos et al., 2014). In general, total solar insolation promotes cirque formation on South- and North-facing slopes, in the Southern and Northern hemispheres, respectively. In contrast, prevailing winds promote cirque development on lee slopes, where snow and ice redistributed from up-wind slopes accumulates, and is protected from deflation (Evans, 1977; Evans, 1990). These impacts on cirque aspect are often most apparent where glaciation is marginal (i.e., where the topography extends just above the regional equilibrium line altitude, ELA), meaning that glaciers are only able to form on climatically favourable slopes (Barr and Spagnolo, 2015). In such cases, the aspect bias in resulting cirque populations is often particularly strong, and reflected by a high VS (see Evans, 1977). By contrast, in the TAM, it is notable that VS is very low (Fig. 7). This might reflect the fact that Cenozoic glaciation in Antarctica has been extensive, often covering most of the continent (Anderson et al., 2002), meaning that cirque-forming glaciers were able to develop on slopes with a range of aspects. It is also apparent that none of the cirque populations in the TAM show an overall aspect bias (as reflected by the VM) towards the south (Fig. 3a & b). The lack of a southerly aspect bias likely indicates that total solar insolation was not a key control on where glaciers were able to initiate in the TAM. This might reflect the region's high latitude, where Sun angles during the ablation season (i.e., Austral summer) are such that aspect-related contrast in the receipt of solar insolation on slopes are minimal when compared to lower latitudes. Similarly weak aspect bias is observed for populations of high latitude modern glaciers, e.g., glacier populations in Novaya Zemlya (~74°N), SE Ellesmere Island (~77°N), Svalbard (~78°N), Axel Heiberg Island (~79°N), Severnaya Zemlya (78–81°N), and Franz Jozef Land (80–83°N) have relatively low VS of 23 %, 23 %, 21 %, 7 %, 33 %, and 31 % respectively (Evans, 2006a). In addition, Evans and Cox (2005) demonstrate that for modern glaciers, little N-S altitude asymmetry is expected between 70° (N or S) and the Pole, indicating the negligible role that aspect-related contrasts in the receipt of solar insolation play in regulating glacier locations at such latitudes.

Though there is no southerly cirque aspect bias in the TAM, the population as a whole and each of the sub-populations show some aspect bias towards the North, NW, or NE (Fig. 3a & b), suggesting that prevailing wind directions may have played the dominant role in regulating on which slopes glaciers and therefore cirques were most readily able to form. At present, the prevailing winds in the TAM are katabatic (Parish and Bromwich, 1987), and flow radially towards the coast (with winds directions partly governed by the topography of the underlying ice) (Fig. 3c) from the centre of the East Antarctic Ice Sheet (EAIS) where they are generated by radiative cooling of air masses (Parish and

Table 5
Cirque aspect vector strength (VS) data for different populations globally. These data are presented in Fig. 7. Data from the present study (i.e., 1,292 glacier-free cirques in the TAM) are displayed in red. Citations for each study: (1) Li et al. (2023); (2) Present study; (3) Li et al. (2023); (4) Li et al. (2023); (5) Zhang et al. (2020); (6) Gâștescu (1971); (7) Li et al. (2023); (8) Zhang et al. (2021); (9) Pippan (p.c.); (10) Urdea (2001); (11) Löeffler (1972); (12) Sale (1970); (13) Niculescu (1965); (14) Péwé et al. (1967); (15) Atwood (1909); (16) Oien et al. (2022); (17) Sale (1970); (18) McLaren and Hills (1973); (19) Hassinen (1998); (20) Graf (1976); (21) Mîndrescu et al. (2010); (22) Derbyshire (p.c.); (23) Schmidt-Thomé (1973); (24) Harker (1901); (25) Gâștescu (1971); (26) Sale (1970); (27) Ivanovskiy (1965); (28) Porter (p.c.); (29) Oien et al. (2022); (30) Wojciechowski and Wilgat (1972); (31) Goldthwait (1970); (32) Salisbury (1901); (33) Gâștescu (1971); (34) Li et al. (2023); (35) Barr and Spagnolo (2013); (36) Andrews et al. (1970); (37) Barr et al. (2017); (38) Soyez (1974); (39) Temple (1965); (40) Rudberg (1954); (41) Spencer (1959); (42) Whitaker (p.c.); (43) Andrews et al. (1970); (44) Godard (1965); (45) Mutch (1963); (46) Schmitz (1969); (47) Sissons (1967); (48) Evans (1999); (49) Clough, 1974, Clough, 1977; (50) Evans (1994); (51) Derbyshire and Evans (1976); (52) Gordon (1977); (53) Unwin (1973); (54) Sugden (1969); (55) Evans (2006a); (56) Oberbeck (1964); (57) Evans (1974); (58) Evans and Cox (1995); (59) Evans (1974); (60) Ergenzinger (1967); (61) Kornilov (1964); (62) Bain (p.c.); (63) Helland (1877); (64) Evans (1974); (65) Moller and Sollid (1973) (& p. c.); (66) Evans et al. (2021); (67) Evans (1974); (68) King and Gage (1961); (69) Moller and Sollid (1973) (& p. c.); (70) Sale (1970); (71) Pippan (1967); (72) Schmidt-Thomé (1973); (73) Helland (1877); (74) Kłapyta et al. (2023); (75) Lewis (1970); (76) Clapperton (1971); (77) Péwé et al. (1967); (78) Zienert and Fezer (1967); (79) Andrews (1965); (80) Sharp (1960) (& p.c.); (81) Ellis-Grufydd (p.c.); (82) Seddon (1957); (83) Galloway (1963); (84) Fränzle (1959); (85) Evans (1974); (86) Bashenina (1971); (87) Clark (1972); (88) Ivanovskiy (1965); (89) Abele (1964); (90) Sawicki (1911); (91) Ivanovskiy (1965); (92) Dort (1962); (93) Sharp et al. (1959).

Study Number	Region	Number of cirques analysed	Aspect vector mean (°)	Aspect vector strength (%)
1	Central Himalayas	456	039	8
2	Transantarctic Mountains	1292	002	11
3	Southern Altai	535	066	14
4	Eastern Tian Shan	675	020	14
5	Gangdise Mountains, southern Tibetan Plateau	1652	023	16
6	Fagaras, Southern Romania	133	064	18
7	Western Gangdise	562	356	19
8	Central Tibetan Plateau	70	019	20
9	Norway	132	018	22
10	Retezat Mountains, Transylvanian Alps, Romania	31	035	23
11	Papua-New Guinea	182	183	24
12	Scotland	876	044	24
13	Godeanu, Southern Romania	69	106	24
14	Yukon-Tanana upland, Alaska	1087	001	25
15	Wasatch Mountains, Utah	64	337	25
16	Northern Scandinavia	2947	036	27
17	Cumbria, England	104	062	28
18	Eastern Banff National Park, Alberta	53	027	29
19	Northern Scandinavia	539	040	30
20	Rocky Mountains, USA	240	068	30
21	Romania	631	063	31
22	Sierra Nevada, California	85	035	31
23	Orense/Minho border area, Portugal and Spain	36	349	32
24	Cuillin, Scotland	52	018	32
25	Retezat, Southern Romania	48	020	33
26	North Wales	118	059	33
27	Katun Khr., Altai, Southern Siberia	390	027	33
28	Snoqualmie Pass, Washington	189	033	33
29	Southern Scandinavia	1037	033	35
30	Rio Aconcagua area, Chile	112	168	37

31	Presidential Range & Mt. Katahdin, New England	20	076	41
32	Santa Fe Mountains, New Mexico	50	073	42
33	Paring, Southern Romania	40	053	45
34	Northern Altai	603	057	46
35	Kamchatka, Russia	3520	006	46
36	Okoa Bay, Arctic Canada	159	021	46
37	Britain and Ireland	2208	049	47
38	South Lapland	112	116	47
39	West-Central Cumbria, England	73	040	47
40	Västerbotten, Sweden	93	125	47
41	Cumbria, England	67	053	49
42	Cumbria England	102	047	49
43	Home Bay, Arctic Canada	79	036	51
44	NW Scotland	437	048	51
45	Oamaru area, New Zealand	104	100	52
46	Galicia and W. León, Spain	151	049	53
47	Scotland	347	047	54
48	Wales	228	047	55
49	Cumbria, England	198	051	55
50	Cayoosh Range, British Columbia	198	011	56
51	Bendor Range, British Columbia	186	012	56
52	Kintail-Aifric-Cannich, NW Scotland	260	051	57
53	Snowdonia, NW Wales	81	048	57
54	Cairngorms, Scotland	30	047	57
55	Wales	260	049	58
56	Faroe Islands	154	068	58
57	Northern Garibald, British Columbia	193	006	59
58	English Lake District	158	049	60
59	Tatlow Range, British Columbia	71	009	60
60	Böhmerwald, Germany	19	064	60
61	Suntar-Khayata, Eastern Siberia	233	353	60
62	Torridon (north), Scotland	30	031	60
63	Jostedalsbreen, Southern Norway	41	016	61
64	Custer Range, British Columbia	38	001	62
65	Andöya & Langöya, Northern Norway	89	042	63
66	SW Turkey	85	015	64
67	Bridge River area, British Columbia	538	009	64
68	Brandon peninsula, SW Ireland	34	027	64
69	Grytöya, Northern Norway	33	141	65
70	South Wales	15	030	65

71	Cumbria, England	28	047	65
72	Spain	11	037	66
73	Jotunfjelds, Southern Norway	37	012	66
74	Eastern Carpathians	214	038	67
75	Brecon Beacons, Wales	13	044	67
76	Falkland Islands	62	077	68
77	Yukon-Tanana upland, Alaska	387	017	68
78	Vosges & Schwarzwald, Central Europe	179	064	68
79	Northern Nain-Okak, Labrador, Canada	29	029	68
80	Trinity Alps, California	33	010	69
81	South Wales	25	022	71
82	Snowdonia, NW Wales	34	045	72
83	Snowy mountains, Australia	13	124	73
84	Sa. de Guadarrama and Somosierra, Spain	27	106	74
85	Central Japan	22	070	77
86	Khr. Svidoyvets, Ukranian Carpathians	16	052	77
87	Falkland Islands	24	090	79
88	En.Terek Khr., Altai, Southern Siberia	97	028	80
89	Lorea and Mieminger groups, Austria	20	028	80
90	Maramureş Carpathian, Northern Romania	14	055	83
91	Aygulak Khr., Altai, Southern Siberia	43	039	88
92	Coer d'Alene, Idaho	39	013	90
93	San Bernardino, California	9	024	91

Pre-1981 data from Evans (1977). p.c. is personal communication in Evans (1977).

Bromwich, 1987, 2007; Parish and Cassano, 2003; van Lipzig et al., 2004). The aspect data for many of the cirques in each of the sub-regions of the TAM suggests that similar wind patterns prevailed when they were being formed – i.e., in each sub-region the cirque VM is roughly aligned (lies 180°) to the prevailing wind direction (Table 1, and compare Figs. 3 a & b with Fig. 3c). This suggests that the EAIS was present (in some form) at the time of formation of many, though not necessarily all, cirques. The EAIS formed ~34 Ma (DeConto and Pollard, 2003) and was likely centred over the Gamburtsev Mountains (Bo et al., 2009), >1000 km from the TAM (Fig. 2a). However, some of the highest, and therefore oldest (i.e. those that were the first to be occupied by glaciers), cirques in the TAM may have formed 60 Ma ago (Barr et al., 2022). This implies that cirque formation occurred in different regions at different times, in some cases perhaps separated by many millions of years. This is potentially demonstrated when cirque aspect is considered by altitude, i.e., by separating the entire cirque population into ten discrete altitudinal groups (each containing 1406 cirques) data show that as population altitude increases, VS generally decreases, and there is typically more deviation from North-facing aspects (Fig. 8). Specifically, VS is strongest (i.e., >20 %) for the lowest two altitudinal groups of cirques, and < 15 % for the reminder. VM is N in the lowest three altitudinal groups; NE is the next three; and more varied at higher elevations. This might indicate that the highest cirques were generated first, prior to the development of the EAIS (and associated katabatic winds), while the lower altitude cirques formed once the EAIS was in place (and therefore favour North-facing slopes in the lee of katabatic winds).

4.2. Landscape evolution

There is ongoing uncertainty about specifically how and when cirques grow (i.e. are enlarged) and therefore how glaciated mountain landscapes evolve (Crest et al., 2017; Barr et al., 2019; Ruszkiczay-Rüdiger et al., 2021; Salcher et al., 2021). For example, it is possible that cirques are enlarged continuously throughout occupation by glacial ice, or growth may be episodic, with active erosion largely occurring during the initiation and termination of glaciations, when glaciers are small and subglacial erosion is focused within the cirques and promoted by steep and mostly warm/wet-based ice (Barr and Spagnolo, 2013, 2015; Crest et al., 2017). It is also possible that cirques are mostly enlarged during the very early stages of glaciation, and that their dimensions are then altered little during subsequent occupation by glacial ice (Barr et al., 2019; Ruszkiczay-Rüdiger et al., 2021). Results from the present study show that glacier-free cirques in Antarctica are not notably larger than in other regions globally (Fig. 9). Given that some of these Antarctic cirques have been occupied by glacier-ice for millions of years (DeConto and Pollard, 2003; Barr et al., 2022), far longer than in many of these other regions globally (e.g. <140 thousand years for some cirques in British Columbia, see Barr et al., 2019), this seems to indicate that cirque size is not directly linked to the duration of glacier occupation – i.e.

Table 6
Cirque size data for different populations globally. These data are presented in Fig. 9. In each case, values refer to minimum, mean, and maximum for cirque length (L), width (W) and depth (H), all recorded in metres. Data from the present study (i.e., 1,292 glacier-free cirques in the TAM) are displayed in red. Citations for each study: (1) Bathrellos et al. (2014); (2) Ruiz-Fernández et al. (2009); (3) Bathrellos et al. (2014); (4) Gómez-Villar et al. (2015); (5) Bathrellos et al. (2014); (6) Ruiz-Fernández et al. (2009); (7) Pedraza et al. (2019); (8) Delmas et al. (2014); (9) Bathrellos et al. (2014); (10) García-Ruiz et al. (2000); (11) Bathrellos et al. (2014); (12) Lopes et al. (2018); (13) Pedraza et al. (2019); (14) Křížek and Mida (2013); (15) Gómez-Villar et al. (2015); (16) Gordon (1977); (17) Bathrellos et al. (2014); (18) Federici and Spagnolo (2004); (19) Present study; (20) Křížek et al. (2012); (21) Oliva et al. (2020); (22) Hassinen (1998); (23) Barr and Spagnolo (2013); (24) Araos et al. (2018); (25) Wallick and Principato (2020); (26) Li et al. (2023); (27) Steffanová and Mentlík (2007); (28) Marinescu (2007); (29) Aniya and Welch (1981).

Study Number	Region	Number of cirques	L	L	L	W	W	W	H	H	H
1	Peloponnesus, Greece	19	145	253	654	163	442	804	40	145	300
2	Western Massif of Picos de Europa, Spain	59	125	295	475	125	467	1375	119	294	530
3	Sterea Hellas, Greece	63	53	374	2575	149	457	956	40	180	380
4	Montana Central, Cantabrian Mountains, NW Spain	89	168	468	960	192	655	1320	89	237	453
5	Thessaly, Greece	50	159	473	1334	304	731	2468	120	289	640
6	Sierras of Southwest Asturias, Spain	70	125	487	950	250	594	2000	57	255	423
7	Somosierra Mountains (Spain)	18	297	487	971	257	461	754	134	219	498
8	Eastern Pyrenees, France	1071	93	489	1851	99	482	2011	20	223	1070
9	Epirus, Greece	68	137	502	1797	166	766	2146	80	308	900
10	Central Spanish Pyrenees	206	100	519	1600	200	691	2700	100	364	943
11	Crete, Greece	17	162	524	905	290	489	837	20	179	540
12	Central Pyrenees (Aran and Boí valleys)	186	114	528.6	1821	57.2	344	1213	67	393	947
13	Guadarrama Mountains (Spain)	79	172	556	1498	105	530	1751	44	213	516
14	High Tatra, Slovakia and Poland	116	179	570	1961	206	550	1905	103	311	603
15	Upper Sil River basin, Cantabrian Mountains, NW Spain	67	589	625	1286	213	707	1821	118	277	477
16	Kintail-Affric-Cannich, NW Scotland	231	100	625	1840	130	586	2250	92	276	670
17	Macedonia region, Greece	48	195	630	1779	320	702	2212	60	263	700
18	Western French-Italian Alps	432	233	672	2410	211	663	2906	87	355	1328
19	Transantarctic Mountains	1292	199	779	2445	138	833	3170	79	413	1271
20	Czech Republic, Germany, and Poland	27	278	788	1798	360	700	1467	116	272	453
21	Western Fuegian Andes of Argentina	251	140	812	2530	160	809	2580	80	332	836
22	Norway, Sweden, Finland	539	150	845	4000	250	888	3100	90	400	1180
23	Kamchatka, Russia	3520	125	868	2110	250	992	2601	60	421	983
24	Sierra Baguales Mountain Range of southern Patagonia	143	210	870	2520	350	1010	3000	94	320	737
25	Faroe Islands	116	261	950	2301	285	890	2085	91	404	716
26	High Mountain Asia	2831	283	1028	3341	259	945	2528	126	444	2281
27	Czech Republic, Germany	7	677	1040	1237	608	949	1352	187	287	385
28	Gilort Basin, Romania	10	839	1172	1727	589	1124	2549	230	358	490
29	Victoria Valley System (Dry Valleys), Antarctica	56	660	2116	4584	840	1679	3240	314	515	849

cirques don't continuously grow when occupied by glacial ice. There are several reasons to suspect this. First, when glaciation is extensive (as in Antarctica) cirques may become occupied by cold-based, minimally erosive ice (Näslund, 1997; Hassinen, 1998). Second, as cirques over-deepen, sediment may become trapped subglacially, protecting the underlying bed from erosion (Hooke, 1991; Gądek et al., 2015). Third, cirques may grow until they reach a 'least resistance' shape after which bedrock erosion is minimal (Barr et al., 2019). However, our data do show some spatial variability in cirque size across the TAM, a general increase in cirque size with altitude (Table 3), and a tendency for NE-facing cirques to be larger than those facing South (Table 4). A possible explanation for these size differences might be related to ice occupation time, including by the ice sheet, and/or reflect differences in the dynamics of former glaciers (e.g., Delmas et al., 2015). This is particularly true of size variability with aspect, which might relate to differences in the dynamics of former glaciers. For example, on NE-facing slopes the small mountain glaciers that are often presumed to drive cirque development may have been more dynamic (with higher mass-turnover) and therefore more erosive than those on South-facing slopes. The rationale for expecting more dynamic glaciers on these slopes is that the total annual receipt of solar insolation is greatest on North-facing slopes (in the TAM), and glaciers may therefore have experienced more melting than those facing South. In addition, as outlined in Section 4.1., NE-facing glaciers may have experienced more accumulation than South-facing examples since katabatic winds (Fig. 3c) are likely to have re-distributed snow and ice from South-facing slopes and deposited this material on those facing North. This combination of comparatively high melt rates and high accumulation rates on North-facing slopes in the TAM may have resulted in particularly dynamic and erosive glaciers (with steep mass balance gradients) which were able to develop larger cirques.

5. Conclusions

In this study, we conduct the first systematic morphometric analysis of cirques in the Transantarctic Mountains to yield information about past glacier formation and landscape evolution. The main study findings are:

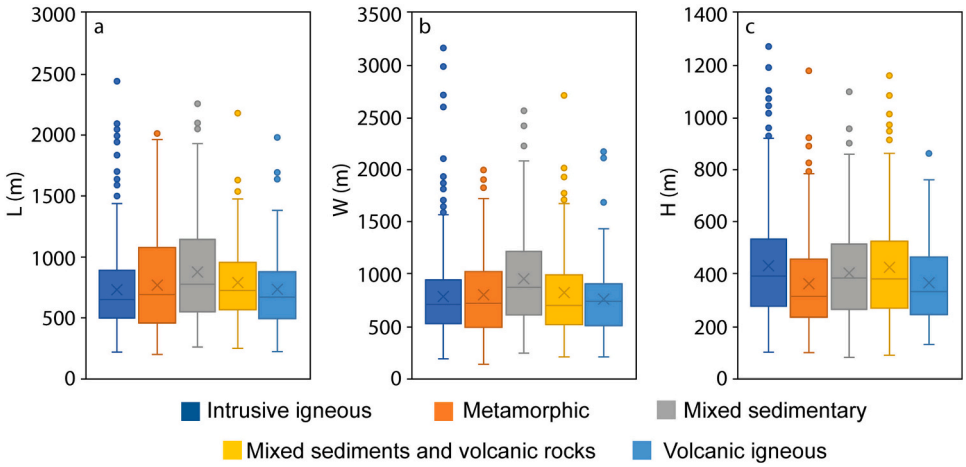

Fig. 6. Variations in the Length (L), Width (W) and depth (H) of glacier-free cirques in the Transantarctic Mountains according to differences in dominant lithology (i.e., the geological unit which accounts for most of a cirque's surface area). Each boxplot shows the median (horizontal line), mean (cross), 1st and 3rd quartiles, and outliers (i.e. values >1.5 box lengths beyond the interquartile range).

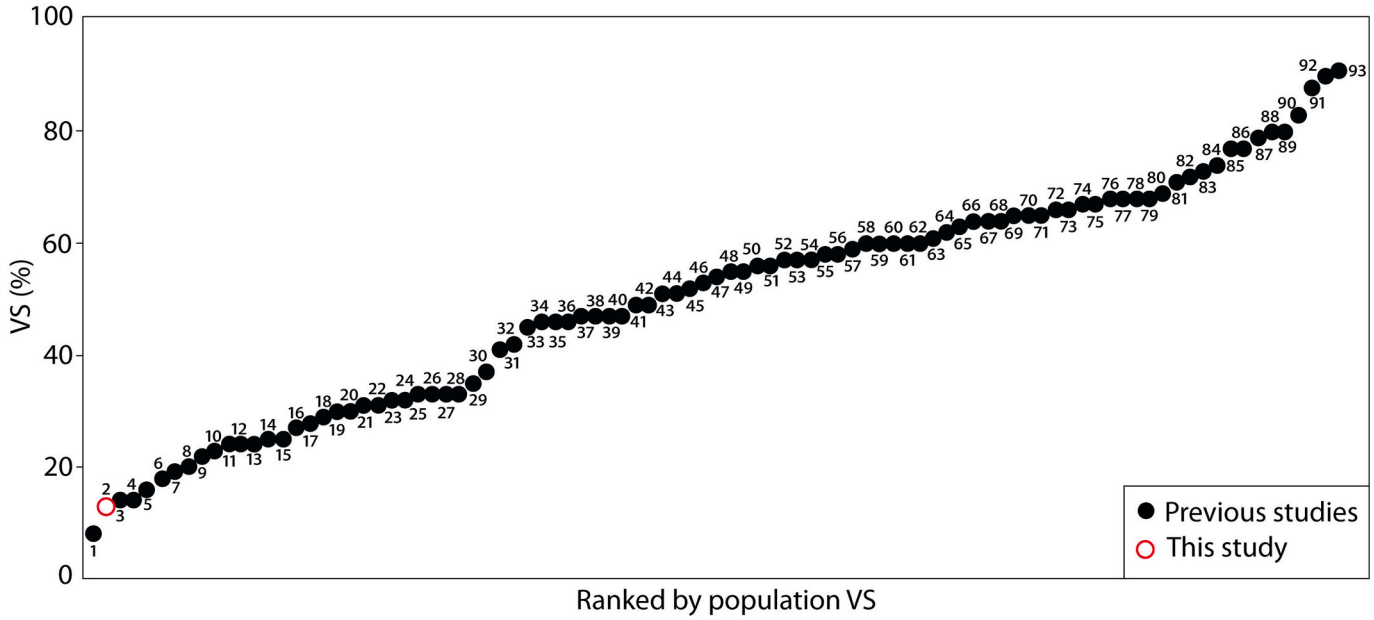

Fig. 7. Cirque aspect vector strength (VS) data for different populations globally. Numbers refer to different studies (details are provided in Table 5). Data from the present study (i.e., all 14.060 cirques in the TAM) are displayed in red (circle with hollow centre).

1. Across the TAM, when glacier-free and glacier-occupied cirque populations are compared, VM and VS are similar, however neither shows a particularly strong aspect bias (as reflected by VS). This likely reflects Antarctica's climate which has been conducive to extensive and widespread glaciation for many millions of years (Miller et al., 2005; Barr et al., 2022), allowing glaciers to form and thereby generate cirques on slopes with a variety of aspects.
2. The lack of a southerly cirque aspect bias indicates that total solar insolation was not a key control on where former glaciers in the TAM were able to initiate, perhaps because of the region's high latitude, where the aspect-related contrasts in the receipt of solar insolation during the ablation season are minimal when compared to lower latitudes.
3. Where cirques in the TAM show some aspect bias, this is typically towards the North, NW and/or NE. This likely reflects the dominant role of prevailing wind directions in controlling the slopes on which past glacier development was favoured. If so, this suggests that during the formation of some cirques, prevailing wind directions in the TAM were similar to present, i.e., dominated by katabatic winds which flow from the interior of the EAIS. This implies that the EAIS was present (in some form) at the time, meaning that many of these cirques are no older than 34 Ma. By contrast, the very highest (and likely oldest) cirques in the TAM have more varied aspects, indicating that they may have formed before katabatic winds came to dominate (therefore sometime prior to 34 Ma, and perhaps as far back as 60 Ma, Barr et al., 2022).
4. In general, we find that cirques in the TAM have similar dimensions to those in other regions globally, despite having been occupied by glacial ice for far longer. Thus, our findings support a growing body

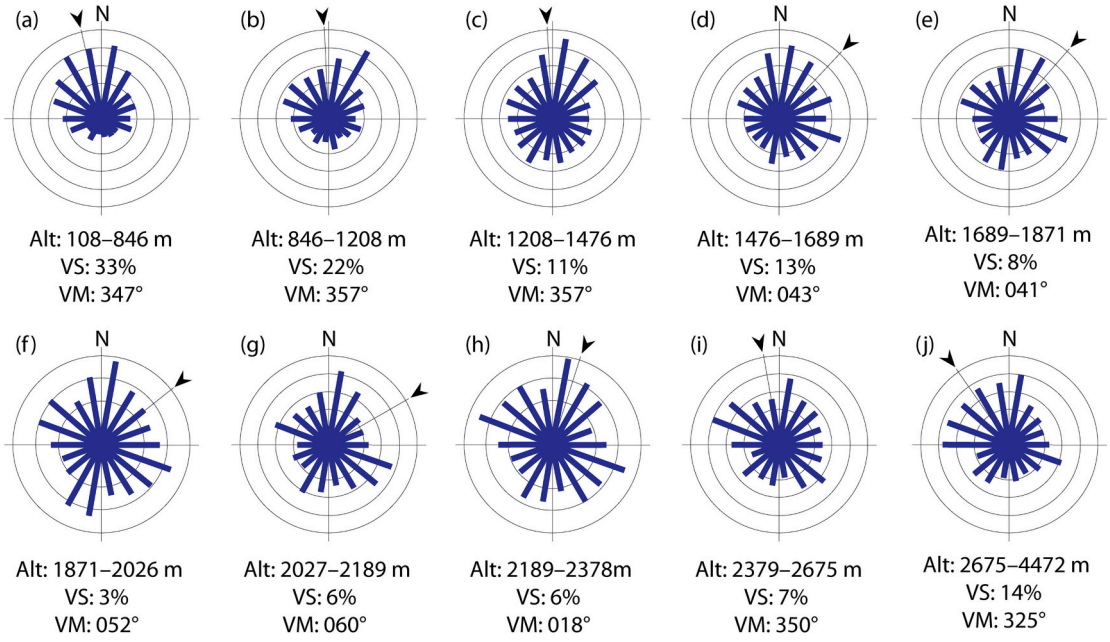

Fig. 8. Aspect data for all 14,060 cirques in the TAM grouped according to their altitude (Z_max). Groups range from (a) the lowest 1406 cirques to (j) the highest. In each image, the arrow corresponds to the Vector Mean (VM).

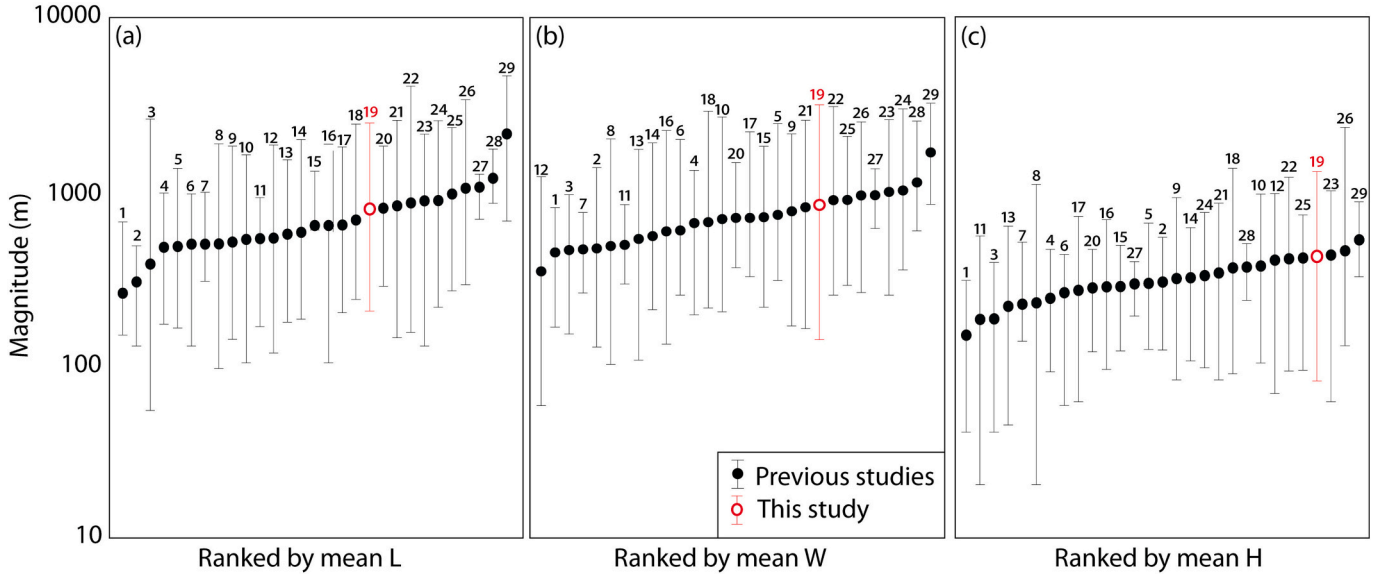

Fig. 9. Cirque size data for different populations globally. Numbers refer to different studies (details are provided in Table 6). Data from the present study (i.e., 1292 glacier-free cirques in the TAM) are displayed in red (circle with hollow centre). (a) Length. (b) Width. (c) depth. Note that the y-axis is logarithmic. Mean, maximum and minimum values are shown here.

of evidence which suggests that cirque size and glacier occupation times are not directly coupled.

5. There is some evidence of variability in cirque size which might reflect differences in ice occupation time and/or relate to the differences in the dynamics of former glaciers, i.e., glaciers on slopes with North, NW and NE aspects (with high mass turnover) were likely more erosive and therefore able to generate larger cirques than minimally erosive glaciers (with comparatively low mass turnover) on other aspects.

Declaration of competing interest

The authors declare that they have no known competing financial interests or personal relationships that could have appeared to influence the work reported in this paper.

Data availability

Data will be made available on request.

Acknowledgements

DEMs provided by the Byrd Polar and Climate Research Center and the Polar Geospatial Center under NSF-OPP awards 1543501, 1810976, 1542736, 1559691, 1043681, 1541332, 0753663, 1548562, 1238993 and NASA award NNX10AN61G. Computer time provided through a Blue Waters Innovation Initiative. DEMs produced using data from DigitalGlobe, Inc. We thank Ian Evans and an anonymous reviewer for their helpful corrections, comments and suggestions.

Appendix A. Supplementary data

Supplementary data associated with this article can be found in the online version, at https://doi.org/10.1016/j.geomorph.2023.108970. These data include the Google maps of the most important areas described in this article.

References

Abele, G., 1964. Die Fernpasstalung und ihre morphologischen Probleme. Tübinger Geogr, Studien, Ht, p. 12.

Anderson, J.B., Shipp, S.S., Lowe, A.L., Wellner, J.S., Mosola, A.B., 2002. The Antarctic Ice Sheet during the last Glacial Maximum and its subsequent retreat history: a review. Quat. Sci. Rev. 21 (1–3), 49–70. https://doi.org/10.1016/S0277-3791(01)00083-X.

Andrews, J.T., 1965. The corries of the northern Nain-Okak section of Labrador. Geogr. Bull. 7 (2), 129–136.

Andrews, J.T., LeMasurier, W.E., 1973. Rates of Quaternary glacial erosion and corrie formation, Marie Byrd Land, Antarctica. Geology 1 (2), 75–80. https://doi.org/10.1130/0091-7613(1973)1<75:ROQGEA>2.0.CO;2.

Andrews, J.T., Barry, R.G., Drapier, L., 1970. An inventory of the present and past glacierization of Home Bay and Okoa Bay, East Baffin Island, NWT, Canada, and some climatic and palaeoclimatic considerations. J. Glaciol. 9 (57), 337–362. https://doi.org/10.3189/S0022143000022875.

Aniya, M., Welch, R., 1981. Morphometric analyses of Antarctic cirques from photogrammetric measurements. Geogr. Ann. Ser. B 63 (1–2), 41–53. https://doi.org/10.1080/04353676.1981.11880017.

Araos, J.M., Le Roux, J.P., Kaplan, M.R., Spagnolo, M., 2018. Factors controlling alpine glaciations in the Sierra Baguales Mountain Range of southern Patagonia (50° S), inferred from the morphometric analysis of glacial cirques. Andean Geol. 45 (3), 357–378. https://doi.org/10.5027/andgeoV45n3-2974.

Atwood, W.W., 1909. Glaciation of the Uinta and Wasatch Mountains, 61. US Government Printing Office.

Barr, I.D., Spagnolo, M., 2013. Palaeoglacial and palaeoclimatic conditions in the NW Pacific, as revealed by a morphometric analysis of cirques upon the Kamchatka Peninsula. Geomorphology 192, 15–29. https://doi.org/10.1016/j.geomorph.2013.03.011.

Barr, I.D., Spagnolo, M., 2015. Glacial cirques as palaeoenvironmental indicators: their potential and limitations. Earth Sci. Rev. 151, 48–78. https://doi.org/10.1016/j.earscirev.2015.10.004.

Barr, I.D., Ely, J.C., Spagnolo, M., Clark, C.D., Evans, I.S., Pellicer, X.M., Pellitero, R., Rea, B.R., 2017. Climate patterns during former periods of mountain glaciation in Britain and Ireland: Inferences from the cirque record. Palaeogeogr. Palaeoclimatol. Palaeoecol. 485, 466–475. https://doi.org/10.1016/j.palaeo.2017.07.001.

Barr, I.D., Ely, J.C., Spagnolo, M., Evans, I.S., Tomkins, M.D., 2019. The dynamics of mountain erosion: cirque growth slows as landscapes age. Earth Surf. Process. Landf. 44 (13), 2628–2637. https://doi.org/10.1002/esp.4688.

Barr, I.D., Spagnolo, M., Rea, B.R., Bingham, R.G., Oien, R.P., Adamson, K., Ely, J.C., Mullan, D.J., Pellitero, R., Tomkins, M.D., 2022. 60 million years of glaciation in the Transantarctic Mountains. Nat. Commun. 13 (1), 5526. https://doi.org/10.1038/s41467-022-33310-z.

Bashenina, N.V., 1971. O roli blokovoy morfotektoniki v oledenenii sovetskikh Karpat. Izvestiya Vsesoyuznogo Geograficheskogo Obshchestva 103 (2), 166–170.

Bathrellos, G.D., Skilodimou, H.D., Maroukian, H., 2014. The spatial distribution of Middle and late Pleistocene cirques in Greece. Geogr. Ann. Ser. B 96 (3), 323–338. https://doi.org/10.1111/geoa.12044.

Bo, S., Siegert, M.J., Mudd, S.M., Sugden, D., Fujita, S., Xiangbin, C., Yunyun, J., Xueyuan, T., Yuansheng, L., 2009. The Gamburtsev mountains and the origin and early evolution of the Antarctic Ice Sheet. Nature 459 (7247), 690–693. https://doi.org/10.1038/nature08024.

Clapperton, C.M., 1971. Evidence of cirque glaciation in the Falkland Islands. J. Glaciol. 10 (58), 121–125. https://doi.org/10.3189/S0022143000013058.

Clark, R., 1972. Periglacial landforms and landscapes in the Falkland Islands. Biul. Peryglac. 21, 33–50.

Clough, R.M., 1974. The Morphology and Evolution of the Lakeland Corries. Unpublished M. Phil, dissertation in Geography, Queen Mary College. University of London, England.

Clough, R.M., 1977. Some aspects of corrie initiation and evolution in the English Lake District. Proceedings, Cumberland Geological Society 3, 209–232.

Cox, S.C., Smith Lyttle, B., Elkind, S., Smith Siddoway, C., Morin, P., Capponi, G., Abu-Alam, T., Ballinger, M., Bamber, L., Kitchener, B., Lelli, L., 2023. A continent-wide detailed geological map dataset of Antarctica. Scientific Data 10 (1), 250. https://doi.org/10.1038/s41597-023-02152-9.

Crest, Y., Delmas, M., Braucher, R., Gunnell, Y., Calvet, M., Aster Team, 2017. Cirques have growth spurts during deglacial and interglacial periods: evidence from 10Be and 26Al nuclide inventories in the central and eastern Pyrenees. Geomorphology 278, 60–77. https://doi.org/10.1016/j.geomorph.2016.10.035.

DeConto, R.M., Pollard, D., 2003. Rapid Cenozoic glaciation of Antarctica induced by declining atmospheric CO2. Nature 421 (6920), 245–249. https://doi.org/10.1038/nature01290.

Delmas, M., Gunnell, Y., Calvet, M., 2014. Environmental controls on alpine cirque size. Geomorphology 206, 318–329. https://doi.org/10.1016/j.geomorph.2013.09.037.

Delmas, M., Gunnell, Y., Calvet, M., 2015. A critical appraisal of allometric growth among alpine cirques based on multivariate statistics and spatial analysis. Geomorphology 228, 637–652. https://doi.org/10.1016/j.geomorph.2014.10.021.

Derbyshire, E., Evans, I.S., 1976. The climatic factor in cirque variation. In: Derbyshire, E. (Ed.), Geomorphology and Climate. John Wiley & Sons, Chichester, pp. 447–494.

Dort Jr., W., 1962. Glaciation of the Coeur d'Alene District, Idaho. Geol. Soc. Am. Bull. 73 (7), 889–906. https://doi.org/10.1130/0016-7606(1962)73[889:GOTCDD]2.0.CO;2.

Elliot, D.H., 2013. The geological and tectonic evolution of the Transantarctic Mountains: a review. Geol. Soc. Lond. Spec. Publ. 381 (1), 7–35. https://doi.org/10.1144/SP381.14.

Ergenzinger, P., 1967. Die eiszeitliche Vergletscherung des Bayerischen Waldes. E&G Quaternary Sci. J. 18, 152–168. https://doi.org/10.3285/eg.18.1.10.

Evans, I.S., 1974. The Geomorphometry and Asymmetry of Glaciated Mountains (with Special Reference to the Bridge River District, British Columbia). Unpublished Ph.D. Dissertation,. University of Cambridge.

Evans, I.S., 1977. World-wide variations in the direction and concentration of cirque and glacier aspects. Geogr. Ann. Ser. B 59 (3–4), 151–175. https://doi.org/10.1080/04353676.1977.11879949.

Evans, I.S., 1990. Climatic effects on glacier distribution across the Southern Coast Mountains. BC, Canada. Ann. Glaciol. 14, 58–64. https://doi.org/10.3189/S0260305500008272.

Evans, I.S., 1994. Lithological and structural effects on forms of glacial erosion: Cirques and lake basins. In: Robinson, D.A., Williams, R.B.G. (Eds.), Rock Weathering and Landform Evolution. John Wiley & Sons Ltd., Chichester, pp. 455–472.

Evans, I.S., 1999. Was the cirque glaciation of Wales time-transgressive, or not? Ann. Glaciol. 28, 33–39. https://doi.org/10.3189/172756499781821652.

Evans, I.S., 2006a. Allometric development of glacial cirque form: geological, relief and regional effects on the cirques of Wales. Geomorphology 80 (3–4), 245–266. https://doi.org/10.1016/j.geomorph.2006.02.013.

Evans, I.S., 2006b. Local aspect asymmetry of mountain glaciation: a global survey of consistency of favoured directions for glacier numbers and altitudes. Geomorphology 73 (1–2), 166–184. https://doi.org/10.1016/j.geomorph.2005.07.009.

Evans, I.S., Cox, N.J., 1995. The form of glacial cirques in the English Lake District, Cumbria. Z. Geomorphol. 175–202. https://doi.org/10.1127/zfg/39/1995/175.

Evans, I.S., Cox, N.J., 2005. Global variations of local asymmetry in glacier altitude: separation of north–south and east–west components. J. Glaciol. 51 (174), 469–482. https://doi.org/10.3189/172756505781829205.

Evans, I.S., Cox, N.J., 2017. Comparability of cirque size and shape measures between regions and between researchers. Zeitschrift für Geomorphologie. Supplementary issues. 61 (2), 81–103. https://doi.org/10.1127/zfg_suppl/2016/0329.

Evans, I.S., Çılğın, Z., Bayrakdar, C., Canpolat, E., 2021. The form, distribution and palaeoclimatic implications of cirques in Southwest Turkey (Western Taurus). Geomorphology 391, 107885. https://doi.org/10.1016/j.geomorph.2021.107885.

Federici, P.R., Spagnolo, M., 2004. Morphometric analysis on the size, shape and areal distribution of glacial cirques in the Maritime Alps (Western French-Italian Alps). Geogr. Ann. Ser. B 86 (3), 235–248. https://doi.org/10.1111/j.0435-3676.2004.00228.x.

Fränzle, O., 1959. Glaciale und periglaciale Formbildung in Östlichen Kastilischen Scheidegebirge (Zentral spanien). Bonner Geogr. Abh., Ht, p. 26.

Fretwell, P., et al., 2013. Bedmap2: improved ice bed, surface and thickness datasets for Antarctica. Cryosphere 7 (1), 375–393. https://doi.org/10.5194/tc-7-375-2013.

Gądek, B., Grabiec, M., Kędzia, S., 2015. Application of ground penetrating radar to identification of thickness and structure of sediments in postglacial lakes, illustrated with an example of the Mały Staw lake (the Karkonosze Mountains). Studia Geomorphologica Carpatho-Balcanica 49 (1), 5–13. https://doi.org/10.1515/sgcb-2015-0006.

Galloway, R.W., 1963. Glaciation in the Snowy Mountains: a reappraisal. Proc. Linnean Soc. NSW 88 (2), 180–198.

García-Ruiz, J.M., Gómez-Villar, A., Ortigosa, L., Martí-Bono, C., 2000. Morphometry of glacial cirques in the central Spanish Pyrenees. Geogr. Ann. Ser. B 82 (4), 433–442. https://doi.org/10.1111/j.0435-3676.2000.00132.x.

Gâștescu, P., 1971. Lacurile din România: limnologie regională. Editura Academiei Republicii Socialiste România.

Gerrish, L., Fretwell, P., Cooper, P., 2021. Medium resolution vector polygons of the Antarctic coastline (7.4) [Data set]. UK Polar Data Centre, Natural Environment Research Council, UK Research & Innovation. https://doi.org/10.5285/747e63e-9d93-49c2-bafc-cf3d3f8e5afa'.

Godard, A., 1965. Recherches de géomorphologie en Écosse du Nord-Ouest. Les Belles Lettres, Paris.

Goldthwait, R.P., 1970. Mountain glaciers of the Presidential Range in New Hampshire. Arct. Alp. Res. 2 (2), 85–102. https://doi.org/10.1080/00040851.1970.12003566.
Gómez-Villar, A., Santos-González, J., González-Gutiérrez, R.B., Redondo-Vega, J.M., 2015. Glacial cirques in the southern side of the Cantabrian Mountains of southwestern Europe. Geogr. Ann. Ser. B 97 (4), 633–651. https://doi.org/10.1111/geoa.12104.
Goodge, J.W., 2020. Geological and tectonic evolution of the Transantarctic Mountains, from ancient craton to recent enigma. Gondwana Res. 80, 50–122. https://doi.org/10.1016/j.gr.2019.11.001.
Gordon, J.E., 1977. Morphometry of cirques in the Kintail-Affric-Cannich area of Northwest Scotland. Geogr. Ann. Ser. B 59 (3–4), 177–194. https://doi.org/10.1080/04353676.1977.11879950.
Gordon, J.E., 2001. The corries of the Cairngorm Mountains. Scott. Geogr. J. 117 (1), 49–62. https://doi.org/10.1080/00369220118737110.
Graf, W.L., 1976. Cirques as glacier locations. Arct. Alp. Res. 8 (1), 79–90.
Harker, A., 1901. XII.—Ice-Erosion in the Cuillin Hills, Skye. Earth Environ. Sci. Trans. R. Soc. Edinb. 40 (2), 221–252. https://doi.org/10.1017/S008045680003430X.
Hassinen, S., 1998. A morpho-statistical study of cirques and cirque glaciers in the Senja-Kilpisjärvi area, northern Scandinavia. Norsk Geografisk Tidsskrift-Norwegian Journal of Geography 52 (1), 27–36. https://doi.org/10.1080/00291959808552381.
Helland, A., 1877. On the Ice-Fjords of North Greenland, and on the Formation of Fjords, Lakes, and cirques in Norway and Greenland. Q. J. Geol. Soc. 33 (1–4), 142–176. https://doi.org/10.1144/GSL.JGS.1877.033.01-04.1.
Holmlund, P., Näslund, J.O., 1994. The glacially sculptured landscape in Dronning Maud Land, Antarctica, formed by wet-based mountain glaciation and not by the present ice sheet. Boreas 23 (2), 139–148. https://doi.org/10.1111/j.1502-3885.1994.tb00594.x.
Hooke, R.L., 1991. Positive feedbacks associated with erosion of glacial cirques and overdeepenings. Geol. Soc. Am. Bull. 103 (8), 1104–1108. https://doi.org/10.1130/0016-7606(1991)103<1104:PFAWEO>2.3.CO;2.
Howat, I.M., Porter, C., Smith, B.E., Noh, M.-J., Morin, P., 2019. The Reference Elevation Model of Antarctica. Cryosphere 13 (2), 665–674. https://doi.org/10.5194/tc-13-665-2019.
Ivanovskiy, L.N., 1965. Rasprostraneniye, morfologiya i proiskhozhdeniye Karov Altaya. Sibirskiy Geograficheskiy Sbornik 4, 152–198.
Jamieson, S.S., Stokes, C.R., Ross, N., Rippin, D.M., Bingham, R.G., Wilson, D.S., Margold, M., Bentley, M.J., 2014. The glacial geomorphology of the Antarctic ice sheet bed. Antarct. Sci. 26 (6), 724–741. https://doi.org/10.1017/S0954102014000212.
King, C.A.M., Gage, M., 1961. Notes on the extent of glaciation in parts of West Kerry. Ir. Geogr. 4 (3), 202–208. https://doi.org/10.1080/00750776109555545.
Kłapyta, P., Zasadni, J., Mîndrescu, M., 2023. Late Pleistocene glaciation in the Eastern Carpathians–a regional overview. Catena 224, 106994. https://doi.org/10.1016/j.catena.2023.106994.
Kornilov, B.A., 1964. Issledovaniya po marshrutu ot Oymyakonskogo ploskogorya do poberezhya Okhotskogo moray. In: Grave, N.A., et al. (Eds.), Promerzaniye zemnoy poverkhnosti i oledeneniye Khrebta Suntar-Khayata (Vostochnaya Yakutiya). Moskva, Izdatelstvo 'Nauka' (Rezultaty issledovaniy po programme Mezhdunarodnogo Geofizicheskogo Goda). Glyatsiologiya. IX razdel programmy MGG, 14, pp. 106–115.
Křížek, M., Mida, P., 2013. The influence of aspect and altitude on the size, shape and spatial distribution of glacial cirques in the High Tatras (Slovakia, Poland). Geomorphology 198, 57–68. https://doi.org/10.1016/j.geomorph.2013.05.012.
Křížek, M., Vočadlová, K., Engel, Z., 2012. Cirque overdeepening and their relationship to morphometry. Geomorphology 139, 495–505. https://doi.org/10.1016/j.geomorph.2011.11.014.
Lewis, C.A., 1970. The glaciations of the Brecknock Beacons, Wales. Brycheiniog 14, 97–120.
Li, Y., Zhao, Z., Evans, I.S., 2023. Cirque morphology and palaeo-climate indications along a south-north transect in High Mountain Asia. Geomorphology 431, 108688. https://doi.org/10.1016/j.geomorph.2023.108688.
van Lipzig, N.P.M., Turner, J., Colwell, S.R., van Den Broeke, M.R., 2004. The near-surface wind field over the Antarctic continent. Int. J. Climatol. 24 (15), 1973–1982. https://doi.org/10.1002/joc.1090.
Löeffler, E., 1972. Pleistocene glaciation in Papua and New Guinea. Z. Geomorphol. Suppl. 13 (1972), 32–58.
Lopes, L., Oliva, M., Fernandes, M., Pereira, P., Palma, P., Ruiz-Fernández, J., 2018. Spatial distribution of morphometric parameters of glacial cirques in the Central Pyrenees (Aran and Boí valleys). J. Mt. Sci. 15 (10), 2103–2119. https://doi.org/10.1007/s11629-018-4873-x.
Marinescu, E., 2007. The morphometry of the glacial cirques within the Gilort Basin. Analele Universităţii din Craiova. Seria Geografie 10, 5–12.
McLaren, P., Hills, L.V., 1973. Cirque analysis as a method of predicting the extent of a Pleistocene ice advance. Can. J. Earth Sci. 10 (8), 1211–1225. https://doi.org/10.1139/e73-107.
Miller, K.G., Wright, J.D., Browning, J.V., 2005. Visions of ice sheets in a greenhouse world. Mar. Geol. 217 (3–4), 215–231. https://doi.org/10.1016/j.margeo.2005.02.007.
Mîndrescu, M., Evans, I.S., Cox, N.J., 2010. Climatic implications of cirque distribution in the Romanian Carpathians: palaeowind directions during glacial periods. J. Quat. Sci. 25 (6), 875–888. https://doi.org/10.1002/jqs.1363.
Moller, J.J., Sollid, J.L., 1973. Geomorfologisk Kart over Lofoten-Vesterålen. Nor. Geogr. Tidsskr. 27 (3), 195–205.
Mutch, A.R., 1963. Sheet 23 (Oamaru), Geological Map of New Zealand 1:250,000, 1st edition. Department of Scientific and Industrial Research, Wellington, New Zealand.
Näslund, J.O., 1997. Subglacial preservation of valley morphology at Amundsenisen, western Dronning Maud Land, Antarctica. Earth Surf. Process. Landf. 22 (5), 441–455. https://doi.org/10.1002/(SICI)1096-9837(199705)22:5<441::AID-ESP696>3.0.CO;2-4.
Niculescu, G., 1965. Muntii Godeanu: studiu geomor-fologic Bucureşti. Editura Academiei Republicii Populare Romîne.
Oberbeck, G., 1964. Ergebnisse natur- und kulturgeographischer Untersuchungen auf den Färöern. Beitrage zu einer Landerkunde. Jahrb. der Geogr. Ges. zu Hannover für die Jahre 1960 bis 1962, pp. 13–150.
Oien, R., Barr, I.D., Spagnolo, M., Bingham, R.G., Rea, B.R., Jansen, J., 2022. Controls on the altitude of Scandinavian cirques: what do they tell us about palaeoclimate? Palaeogeogr. Palaeoclimatol. Palaeoecol. 600, 111062 https://doi.org/10.1016/j.palaeo.2022.111062.
Oliva, L., Cioccale, M.A., Rabassa, J.O., 2020. Morphometry and spatial distribution of glacial cirques in the Western Fuegian Andes of Argentina, southernmost South America. Andean Geol. 47 (2), 316–350. https://doi.org/10.5027/andgeoV47n2-3188.
Parish, T.R., Bromwich, D.H., 1987. The surface windfield over the Antarctic ice sheets. Nature 328 (6125), 51–54. https://doi.org/10.1038/328051a0.
Parish, T.R., Bromwich, D.H., 2007. Reexamination of the near-surface airflow over the Antarctic continent and implications on atmospheric circulations at high southern latitudes. Mon. Weather Rev. 135 (5), 1961–1973. https://doi.org/10.1175/MWR3374.1.
Parish, T.R., Cassano, J.J., 2003. Diagnosis of the katabatic wind influence on the wintertime Antarctic surface wind field from numerical simulations. Mon. Weather Rev. 131 (6), 1128–1139 doi: 10.1175/1520-0493(2003)131<1128:DOTKWI>2.0.CO;2.
Pedraza, J., Carrasco, R.M., Villa, J., Soteres, R.L., Karampaglidis, T., Fernández-Lozano, J., 2019. Cirques in the Sierra de Guadarrama and Somosierra mountains (Iberian Central System): Shape, size and controlling factors. Geomorphology 341, 153–168. https://doi.org/10.1016/j.geomorph.2019.05.024.
Péwé, T.L., Burbank, L., Mayo, L.R., 1967. Multiple glaciation of the Yukon–Tanana upland, Alaska. United States Geological Survey. Miscellaneous Geologic Investigations Map, 507, p. 1 sheet.
Pippan, T., 1967. Comparative glacio-morphological research in Alpine, Hercynian and Caledonian mountains of Europe. In: Sporck, J.A. (Ed.), Mdlangés de géographie offerts a M. Omer Tulippe, 1, pp. 87–104. Gembloux, Belgique, J. Duculot.
Rose, K.C., Ferraccioli, F., Jamieson, S.S., Bell, R.E., Corr, H., Creyts, T.T., Braaten, D., Jordan, T.A., Fretwell, P.T., Damaske, D., 2013. Early East Antarctic ice sheet growth recorded in the landscape of the Gamburtsev Subglacial Mountains. Earth Planet. Sci. Lett. 375, 1–12. https://doi.org/10.1016/j.epsl.2013.03.053.
Rudberg, S., 1954. Västerbottens Berggrundsmorfologi Geografica. Skrifter från Upsala Univ, Geogr. Inst., p. 25
Ruiz-Fernández, J., Poblete-Piedrabuena, M.A., Serrano-Muela, M.P., Martí-Bono, C., García-Ruiz, J.M., 2009. Morphometry of glacial cirques in the Cantabrian Range (Northwest Spain). Z. Geomorphol. 47–68. https://doi.org/10.1127/0372-8854/2009/0053-0047.
Ruszkiczay-Rüdiger, Z., Kern, Z., Urdea, P., Madarász, B., Braucher, R., ASTER Team, 2021. Limited glacial erosion during the last glaciation in mid-latitude cirques (Retezat Mts, Southern Carpathians, Romania). Geomorphology 384, 107719. https://doi.org/10.1016/j.geomorph.2021.107719.
Salcher, B., Prasicek, G., Baumann, S., Kober, F., 2021. Alpine relief limited by glacial occupation time. Geology 49 (10), 1209–1213. https://doi.org/10.1130/G48639.1.
Sale, C., 1970. Cirque Distribution in Great Britain: A Statistical Analysis of Variations in Elevation, Aspect and Density. Unpublished M.Sc. dissertation. Department of Geography, University College, London.
Salisbury, R.D., 1901. Glacial work in the western mountains in 1901. J. Geol. 9 (8), 718–731.
Sawicki, L.V., 1911. Die glazialen Züge der Rodnaer Alpen und Marmaroscher Karpaten. Mitt. der k.k. Geogr. Ges. zu Wien 54, Ht. 10 and 11, 510–571.
Schmidt-Thomé, P., 1973. Neue, niedrig gelegene Zeugen einer würmeiszeitlichen Vergletscherung in Nordteil der Iberischen Halbinsel (Prov. Vizcaya und Orense in Nordspanien; Minho-Distrikt in Nordportugal). Eiszeitalter u. Gegenwart 23 (24), 384–389.
Schmitz, H., 1969. Glazialmorphologische Untersuchungen im Bergland Nordwestspaniens (Gali-cien/León). Kolner Geogr. Arb., Ht, p. 23.
Seddon, B., 1957. Late-glacial cwm glaciers in Wales. J. Glaciol. 3 (22), 94–99. https://doi.org/10.3189/S0022143000024394.
Selby, M.J., Wilson, A.T., 1971. Possible Tertiary age for some Antarctic cirques. Nature 229 (5287), 623–624. https://doi.org/10.1038/229623a0.
Sharp, R.P., 1960. Pleistocene glaciation in the Trinity Alps of northern California. Am. J. Sci. 258 (5), 305–340. https://doi.org/10.2475/ajs.258.5.305.
Sharp, R.P., Allen, C.R., Meier, M.F., 1959. Am. J. Sci. 257 (2), 81–94. https://doi.org/10.2475/ajs.257.2.81.
Sissons, J.B., 1967. The Evolution of Scotland's Scenery. Oliver and Boyd, Edinburgh.
Small, D., Bentley, M.J., Evans, D.J., Hein, A.S., Freeman, S.P., 2021. Ice-free valleys in the Neptune Range of the Pensacola Mountains, Antarctica: glacial geomorphology, geochronology and potential as palaeoenvironmental archives. Antarct. Sci. 33 (4), 428–455. https://doi.org/10.1017/S0954102021000237.
Soyez, D., 1974. Studien zur Geomorphologie und zum letztglazialen Eisrückzug in den Gebirgen Süd-Lapplands, Schweden. Mit einer Geomorphologischen Übersichtskarte im Masstab 1: 250 000. Geografiska Annaler. Series A. Physical Geography 1–71. https://doi.org/10.2307/520427.
Spagnolo, M., Pellitero, R., Barr, I.D., Ely, J.C., Pellicer, X.M., Rea, B.R., 2017. ACME, a GIS tool for automated cirque metric extraction. Geomorphology 278, 280–286. https://doi.org/10.1016/j.geomorph.2016.11.018.

Spencer, K., 1959. Corrie aspect in the English Lake District. Journal of the Sheffield University Geographical Society 3, 6–9.
Steffanová, P., Mentlík, P., 2007. Comparison of morphometric characteristics of cirques in the Bohemian Forest. Silva Gabreta 13 (3), 191–204.
Sugden, D.E., 1969. The age and form of corries in the Cairngorms. Scott. Geogr. Mag. 85 (1), 34–46. https://doi.org/10.1080/00369226908736110.
Temple, P.H., 1965. Some aspects of cirque distribution in the west-Central Lake District, northern England. Geogr. Ann. Ser. B 47 (3), 185–193. https://doi.org/10.1080/04353676.1965.11879718.
Unwin, D.J., 1973. The distribution and orientation of corries in northern Snowdonia, Wales. Trans. Inst. Br. Geogr. 85–97. https://doi.org/10.2307/621583.
Urdea, P., 2001. Glaciar relief and pleistocene glaciation in Retezat mountains (Transylvanians Alps, Romania). Geographica Pannonica 5, 4–7. https://doi.org/10.5937/GeoPan0105004U.
Wallick, K.N., Principato, S.M., 2020. Quantitative analyses of cirques on the Faroe Islands: evidence for time transgressive glacier occupation. Boreas 49 (4), 828–840. https://doi.org/10.1111/bor.12458.
Wang, Y., Zhang, X., Ning, W., Lazzara, M.A., Ding, M., Reijmer, C.H., Smeets, P.C.J.P., Grigioni, P., Heil, P., Thomas, E.R., Mikolajczyk, D., Welhouse, L.J., Keller, L.M., Zhai, Z., Sun, Y., Hou, S., 2023. The AntAWS dataset: a compilation of Antarctic automatic weather station observations. Earth System Science Data 15 (1), 411–429. https://doi.org/10.5194/essd-15-411-2023.
Wojciechowski, K.H., Wilgat, T., 1972. Mapa geologiczno-hydrograficzna dorzecza górnej Rio Aconcagua. Przeglad Geograficzny 14 (4), 635–648.
Zhang, Q., Fu, P., Yi, C., Wang, N., Wang, Y., Capolongo, D., Zech, R., 2020. Palaeoglacial and palaeoenvironmental conditions of the Gangdise Mountains, southern Tibetan Plateau, as revealed by an ice-free cirque morphology analysis. Geomorphology 370, 107391. https://doi.org/10.1016/j.geomorph.2020.107391.
Zhang, Q., Dong, W., Dou, J., Dong, G., Zech, R., 2021. Cirques of the central Tibetan Plateau: Morphology and controlling factors. Palaeogeogr. Palaeoclimatol. Palaeoecol. 582, 110656 https://doi.org/10.1016/j.palaeo.2021.110656.
Zienert, A., Fezer, F., 1967. Vogesen- und Schwarzwald-Kare. E&G Quaternary Sci. J. 18, 51–75. https://doi.org/10.3285/eg.18.1.02.